DOI: 10.1002/ ((please add manuscript number))
Article type: Full Paper

Programmable Self-Assembling 3D Architectures Generated by Patterning of Swellable MOF-based Composite Films

*Javier Troyano, Arnau Carné-Sánchez, Daniel Maspoch**

Dr. J.T., Dr. A.C., Prof. D.M., Catalan Institute of Nanoscience and Nanotechnology (ICN2), CSIC and the Barcelona Institute of Science and Technology. Campus UAB, Bellaterra, 08193 Barcelona, Spain

Prof. D. Maspoch, ICREA, Pg. Lluís Companys 23, Barcelona, 08010, Spain

Keywords: metal-organic framework, stimuli-responsive, self-folding, smart material, composite film

The integration of swellable MOFs into polymeric composite films is a straightforward strategy to develop soft materials which undergo reversible shape transformations derived from the intrinsic flexibility of MOF crystals. However, a crucial step towards their practical application relies in the ability to attain specific and programmable actuation, which enables the design of

self-shaping objects on demand. Herein, a chemical etching method is demonstrated for the fabrication of patterned composite films showing tunable self-folding response, predictable and reversible 2D-to-3D shape transformations triggered by water adsorption/desorption. These films are fabricated by selective removal of swellable MOF crystals allowing the control over their spatial distribution within the polymeric film. Upon exposure to moisture, various programmable 3D architectures that include a mechanical gripper, a lift and a unidirectional walking device are generated. Remarkably, these 2D-to-3D shape transformations can be reversed by light-induced desorption. The reported strategy offers a platform for fabricating flexible MOF-based autonomous soft mechanical devices with functionalities for micromanipulation, automation and robotics.

Adaptive self-shaping phenomena are ubiquitous in living systems, from unicellular organisms to human beings, and are critical for many biological processes.[1] These morphing mechanisms enable biological structures to autonomously change their shape in response to environmental stimuli (*e.g.* changes in moisture, pH, temperature or light). Artificial systems that could undergo autonomous and controlled shape transformations would have many practical applications; accordingly, the development of such systems, by mimicking the corresponding natural processes, is now a growing field of research.[2, 3] For instance, the development of smart film materials that can self-assemble into well-defined three-dimensional (3D) architectures would offer great potential for energy harvesting,[4] soft-robotics,[5] encapsulation,[6] flexible electronics[7] and medical devices.[8]

_ENREF_12The responsive behavior of self-shaping systems relies on heterogeneous expansion and shrinking, whereby the material is forced to minimize its elastic energy by adopting a preferential configuration. The simplest way to achieve such heterogeneity is via assembly of (multi)bilayers built from components that differ in their swelling properties.[2, 9] However, such bilayer structures typically show weak interfacial adhesion; consequently, they tend to delaminate after repetitive actuation. Moreover, shape-transformations of (multi)bilayers are limited to self-rolling structures (*e.g.* tubes and scrolls), which precludes creation of 3D architectures of greater complexity. Thus, a more convenient approach to design custom morphable 3D objects is to fabricate monolayer materials and control the distribution of swellable and non-swellable (or less swellable) domains. There are various ways to achieve this distribution, including controlling reaction–diffusion processes,[10] localizing oxidative reactions,[11] patterning ions by electric fields[12] or orientating cross-linking in polymers.[13] _ENREF_23

A recent alternative strategy for designing programmed self-shaping monolayers is the fabrication of composite films through embedding of swellable/non swellable materials into a

non-responsive/responsive polymer matrix, respectively.[14] Following this approach, we recently demonstrated that third-generation swellable metal–organic frameworks (MOFs)[15] _ENREF_36 can also be exploited to create humidity-driven self-folding polymer films (**Figure 1**a and Scheme S1, Supporting Information).[16] In these composite films (also known as mixed matrix membranes)[17], the swelling response upon adsorption of heterogeneously distributed MIL-88A (MIL = Materials from Institut Lavoisier) crystals into a PVDF (polyvinylidene difluoride) polymer matrix generates an anisotropic strain over the composite film, causing the composite to fold. However, this approach is restricted to creation of a vertical gradient over the entire film, which limits the film actuation to simple *uniaxial* bending (Scheme S1, Supporting Information). Herein, we extend this concept to develop multi-axial actuated MIL-88A@PVDF films that can undergo programmable and well-defined 2D-to-3D transformations and thus, it enables generation of programmable self-shaping 3D architectures (Figure 1c). We created these films by fabricating patterns of passive (*i.e.* mask-protected) non-folding domains and active (*i.e.* HCl-exposed) self-folding domains of MIL-88@PVDF that can be spatially localized and shaped (Figure 1 b). We also show that, owing to the photothermal effect of MIL-88A crystals, our self-assembled 3D architectures can readily readopt their initial 2D planar shape upon irradiation with UV-Vis light.

-Insert Figure 1-

We began with synthesis of monodisperse MIL-88A crystals, using a surfactant-assisted method.[18] Thus, elongated hexagonal bipyramidal MIL-88A crystals were synthesized by heating a mixture of $FeCl_3 \cdot 6H_2O$, fumaric acid and polyvinylpyrrolidone (PVP) as surfactant in DMF at 85 °C for 2 h (Figure S1, S2, S3 and S4, Supporting Information). These submicrometer-sized MIL-88A crystals (length: 510 ± 125 nm; width:

266 ± 57 nm) were then used to fabricate MIL-88A@PVDF films with a MOF content of 50 wt%, according to a previously reported method (Figure S5, Supporting Information).[16] FESEM analysis revealed formation of a uniform film (thickness: 81 ± 5 μm) with an isotropic distribution of the MIL-88A crystals over the entire film (Figure S6, Supporting Information). Note here that, although embedded MIL-88A crystals retain their reversible swelling behavior (Figure S7 and S8, Supporting Information), their isotropic distribution induces an isotropic strain over the film, due to their expansion/contraction upon solvent adsorption/desorption, which provokes a negligible folding response (Figure S5c, Supporting Information).

We then sought to generate a vertical gradient of MIL-88A crystals embedded within the PVDF film, by chemical etching with HCl vapors. To this end, one side of the fabricated MIL-88A@PVDF films was exposed to an HCl gas flow at room temperature for a period of time (t_e), as depicted in **Figure 2**a (see Experimental Section). After washing with water and ethanol, and drying in air, the exposed side of the film was chalky and whitish, which became more pronounced with longer values of t_e. This color change was the first piece of evidence of progressive, time-dependent removal of MIL-88A crystals (Figure S9, Supporting Information), which was further corroborated by cross-sectional FESEM and energy-dispersive X-ray spectrometry (EDX) studies (Figure S10, S11 and 12, Supporting Information). Figure 2b shows the vertical etching extent (%) as a function of time. A gradual increase in vertical etching was observed, which ranged from 6% at t_e = 1 min to 100% (full etching) at t_e = 20 min.

-Insert Figure 2-

This vertical etching process leads to bilayer PVDF films, in which one layer contains swellable MIL-88A crystals and the other layer does not (Figure 2c). Consequently, upon

exposure to moisture, the etched films self-fold from the side containing the MOF crystals to the etched side (Movie S1, Supporting Information). To evaluate these self-folding properties, we systematically measured the folding angle (φ) of MIL-88A@PVDF strips (length: 3 cm; width: 1 cm) vertically etched at different values of t_e and exposed to 90% relative humidity (RH) for 30 min. Note that, prior to the measurements, each strip was activated at 120 °C for 5 min. As depicted in Figure 2d, the self-folding capacity of the strips increased gradually as the vertical etching increased up to 23% (at t_e = 5 min). However, further increment in the etching led to decrease in the folding response. This trend can be explained by a compromise between two antagonistic effects derived from the etching process. On one hand, the removal of MIL-88A crystals generates a bilayer structure that favors the actuation of the film. On the other hand, as more MOF crystals are removed, the capacity of the MIL-88A@PVDF film to swell upon water adsorption is reduced, causing the loss in performance. In our case, the optimal situation corresponds to a vertical etching of 23% and is characterized by self-rolling behavior with a maximum φ of ~950° at 90% RH (Movie S2, Supporting Information).

We also investigated self-folding behavior of vertically etched MIL-88A@PVDF strips at lower humidity levels. Thus, MIL-88A@PVDF strips with vertical etching values from 6% to 45% were exposed to moisture at relative humidity levels of 20% to 80% (Figure S13, Supporting Information). Figure 2e shows the folding angle of each strip after 30 min of exposure, indicating that the film actuation increased as the relative humidity increased. This trend is consistent with the water isotherm of MIL-88A@PVDF film, which is characterized by a continuous uptake of water over the entire range of relative humidity values (Figure S8, Supporting Information).

Having demonstrated that vertical chemical etching could induce a self-folding response, we next explored fabrication of multi-axial actuated films created from patterns of etched MOF crystals on MIL-88A@PVDF films. To this end, we started with the creation of simple, parallel lines (width: 1 mm) oriented along the length axis, by exposing a MIL-

88A@PVDF strip covered with a predesigned Kapton mask to HCl gas for 5 min. Upon subsequent exposure to 90% RH, the patterned strip folded along its width axis to form an open cylinder (**Figure 3**a and Movie S3, Supporting Information). This expected folding confirmed that patterned lines behave as hinges that guide the folding response of the strip upon water adsorption. To further confirm our control over the self-folding, we changed the orientation of the patterned lines on MIL-88A@PVDF strips to 45° or 90° relative to the length axis. For the MIL-88A@PVDF strip with 45º-lines, exposure to 90% RH provoked a twisting movement, which generated a 3D chiral cylindrical helix. For the MIL-88A@PVDF strip with 90º-lines, exposure to 90% RH caused it to roll along its length axis, leading to formation of another open-cylinder (Figure 3a and Movie S3, Supporting Information).

-Insert Figure 3-

We next used our patterning strategy to build a set of 2D composite films able to transform into programmed 3D architectures (Figure S14, Supporting Information). Firstly, we modified both sides of a square MIL-88A@PVDF film: on one side, we patterned a plus-sign shape, and an another side, an X shape (a plus sign rotated at 45º relative to the plus sign on the other side). Upon exposure to moisture, this patterned square film transformed into a 3D four-pointed star (Figure 3b and Movie S4, Supporting Information). We then created a seven-petal flower-shaped film that, upon exposure to moisture, underwent a reverse-blooming process whereby the active petals folded towards the passive center (Figure 3c and Movie S4, Supporting Information). Remarkably, these heterogeneous MIL-88A@PVDF structures can be employed as water-driven mechanical actuators for specific applications. For instance, the seven-petal flower structure, upon exposure to water, could be used as a mechanical claw to grip a modeling-clay disc 15-times heavier than itself (Figure 4d and Movie S5, Supporting Information). Moreover, a 2D-patterned film comprising four passive

walls connected to a central square area via responsive hinges, was subjected to moisture, causing it to transform into an open cube. The resultant plus sign-shaped structure was used to lift cargo upon exposure to water (Figure 4e). To investigate its load-bearing capacity, the film was loaded with cargo at three different film/cargo weight ratios (1:5, 1:10 and 1:20), and then exposed to 90% RH (Movie S6, Supporting Information). Although increasing weight load led to a slower response time and a less attainable height, the patterned film was still able to lift the cargo at a weight ratio of 1:20.

As we described above, when we exposed our patterned MIL-88A@PVDF films to humidity, they formed programmable 3D architectures -an effect caused by swelling of MIL-88A crystals upon water adsorption. We reasoned that this actuation should be reversible: in other words, that we could cause the 3D architectures to revert back to their initial 2D films by simply removing the adsorbed water molecules from the pores of MIL-88A crystals. In this context, our group has recently demonstrated that solvent molecules can be removed from MOFs by using UV-Vis light for short times and at atmospheric pressure – a consequence of their photothermal effect.[19] To investigate whether this strategy could be used to induce the transformations in our MIL-88A@PVDF structures, we first ascertained whether MIL-88A crystals embedded in the PVDF film could be activated (and thus, shrunk) by exposing the film to UV-Vis light (distance: 4 cm; irradiance: 1590 mW cm^{-2}). Under these conditions, MIL-88A@PVDF film reached a maximum temperature of 103 °C in only 60 s (Figure S15a, Supporting Information). XRPD analysis of this film matched the pattern corresponding to closed-phase MIL-88A, thus confirming evacuation of water from the pores and consequent shrinkage of the crystals (Figure S16, Supporting Information).

Encouraged by the above results, we next evaluated the use of UV-Vis light to reconvert the 3D structures into their corresponding 2D films *in-situ*. To this end, the 3D four-pointed star was irradiated at a distance of ≈ 4 cm, causing the structure to return to its initial flat shape in 120 s (**Figure 4**a). Note that these transformations were reversible: for example,

the reverted flat MIL-88A@PVDF film was reconverted to the 3D four-pointed star upon exposure to moisture (90% RH).

-Insert Figure 4-

Finally, we harnessed our reversible 2D↔3D transformations to develop a MIL-88A@PVDF film that exhibits a unidirectional walking-like movement upon exposure to alternating UV-Vis irradiation under constant relative humidity. For this, we fabricated MIL-88A@PVDF strip (length; 3 cm; width: 1 cm) comprising an active domain (60% of the total length) with 23% vertical etching (t_e = 5 min), and a passive domain (40% of the total length) with a fully-etched region (t_e = 20 min) (Figure 4b). Note that, instead of using a passive domain containing isotropically distributed MIL-88A crystals, we fully etched the crystals to prevent any possible folding of this domain in response to anisotropic heating of MIL-88A crystals caused by irradiation of the polymeric film from above. The resultant MIL-88A@PVDF strip was exposed to on/off cycles of irradiation (on: 5 sec; off: 5 sec) of irradiation at 60% RH, in response to which it exhibited unidirectional motion (Movie S7, Supporting Information). Figure 4c depicts the MIL-88A@PVDF walking mechanism. Initially, the strip bends upward into an arch, due to adsorption of water. Subsequent UV-Vis irradiation causes the active domain of the strip to stretch forward along its longitudinal axis, due to efficient photothermal activation; in contrast, the passive domain acts as a stationary point. When irradiation stopped, the active domain of the strip bends again, upon water adsorption, dragging the passive domain forward and therefore, propelling the strip in one direction.

In summary, we have developed a new strategy for fabrication of programmable self-shaping patterned composite films by controlling the spatial location, in vertical and lateral directions, of swellable MIL-88A crystals within a PVDF polymer matrix. Through controlled

chemical etching, we prepared multiple types of patterned structures, which exhibited enhanced self-folding response and predictable 2D-to-3D shape transformations driven by water adsorption, which we could reverse by light-induced desorption. Such responsive composite films could also serve as autonomous soft mechanical devices, having potential applications in micromanipulation, automation and robotics. Our proposed patterning method provides a simple, fast and low-cost approach to design self-shaping objects with complex geometries and diverse responsive characteristics.

Experimental Section

Materials and Methods: All solvents and reagents were purchased from commercial suppliers and were used without further purification. X-ray powder diffraction (XRPD) patterns under ambient conditions were collected on an X'Pert PRO MPDP analytical diffractometer (Panalytical) at 40 kV and 40 mA using CuKα radiation (λ = 1.5419 Å). The samples were analyzed with scanning θ/2θ. Field-Emission Scanning Electron Microscopy (FESEM) images were collected on a FEI Quanta 650F scanning electron microscope, using aluminum as a support. Gravimetric water vapor sorption isotherms were measured using a DVS vacuum instrument (Surface Measurement Systems Ltd). The weight of the sample (≈ 20 mg) was constantly monitored with a high-resolution microbalance (± 0.1 μg) and recorded at 25 (± 0.2 °C) under pure water vapor pressures. Prior to the sorption experiments, samples were degassed inside the chamber under vacuum at 120 °C for 6 h. Folding angles were calculated as previously described.[16] A Bluepoint 4 ECOcure (Hönle UV Technology) UV-Vis high-intensity spot lamp without a filter (300 nm to 650 nm), and a PI 450 (Optris) infrared camera (operating temperature range: 0 ºC to 250 °C), were used. Data were obtained using PI Connect software.

Synthesis of MIL-88A: A solution of $FeCl_3 \cdot 6H_2O$ (1.35 g, 5 mmol), fumaric acid (0.58 g, 5 mmol) and PVP (1.5 g) in DMF (10 mL) was placed into a glass vial at 85 °C for 2 h. The

resultant brown powder was recovered by centrifugation, washed thoroughly with DMF and methanol, and then, dried at 80 °C.

Preparation of homogeneous MIL-88A@PVDF films: MIL-88A powder (0.125 g) was mixed with PVDF (0.125 g) in DMF (1.25 mL). After sonication for 10 min, the mixture was drop-cast onto a glass slide. Then, the solvent was evaporated off at 140 °C in an oven for approximately 30 min. The resulting film was detached from the substrate by immersion in water, washed thoroughly with ethanol and air-dried.

Preparation of etched MIL-88A@PVDF films: The MIL-88A@PVDF films were attached to a glass substrate with adhesive tape and exposed to an HCl flow for a period of time (t_e). Then, the film was immersed in water, washed thoroughly with ethanol and air-dried. For patterned etched MIL-88A@PVDF films, the designed adhesive Kapton tape-mask was attached to the film surface prior to HCl exposure.

Supporting Information

Supporting Information is available from the Wiley Online Library or from the author.

Acknowledgements

This work was supported by the Spanish MINECO (projects PN MAT2015-65354-C2-1-R), the Catalan AGAUR (project 2014 SGR 80), the ERC under the EU-FP7 (ERC-Co 615954), and the CERCA Program/Generalitat de Catalunya. ICN2 is supported by the Severo Ochoa program from Spanish MINECO (Grant No. SEV-2017-0706).

Received: ((will be filled in by the editorial staff))
Revised: ((will be filled in by the editorial staff))
Published online: ((will be filled in by the editorial staff))

References

[1] a) Y. Forterre, *J. Exp. Bot.* **2013**, *64*, 4745; b) F. Cleri, *The Physics of Living Systems*, Springer, Cham, Switzerland **2016**; c) H.-C. S. Karl J. Niklas, *Plant Physics*, University of Chicago Press, **2012**.

[2] G. Stoychev, S. Zakharchenko, S. Turcaud, J. W. C. Dunlop, L. Ionov, *ACS Nano* **2012**, *6*, 3925.

[3] a) Y. Liu, K. He, G. Chen, W. R. Leow, X. Chen, *Chem. Rev.* **2017**, *117*, 12893; b) L. Suyi, K. W. Wang, *Bioinspiration Biomim.* **2017**, *12*, 011001; c) Y. Liu, J. Genzer, M. D. Dickey, *Prog. Polym. Sci.* **2016**, *52*, 79.

[4] a) X. Guo, H. Li, B. Yeop Ahn, E. B. Duoss, K. J. Hsia, J. A. Lewis, R. G. Nuzzo, *Proc. Natl. Acad. Sci. U.S.A.* **2009**, *106*, 20149; b) R. Liu, X. Kuang, J. Deng, Y.-C. Wang, A. C. Wang, W. Ding, Y.-C. Lai, J. Chen, P. Wang, Z. Lin, H. J. Qi, B. Sun, Z. L. Wang, *Adv. Mater.* **2018**, *30*, 1705195.

[5] G. M. Whitesides, *Angew. Chem. Int. Ed.* **2018**, *57*, 4258.

[6] a) J. Guan, H. He, L. J. Lee, D. J. Hansford, *Small* **2007**, *3*, 412; b) T. S. Shim, S.-H. Kim, C.-J. Heo, H. C. Jeon, S.-M. Yang, *Angew. Chem. Int. Ed.* **2012**, *51*, 1420; c) S. Zhang, A. M. Bellinger, D. L. Glettig, R. Barman, Y.-A. L. Lee, J. Zhu, C. Cleveland, V. A. Montgomery, L. Gu, L. D. Nash, D. J. Maitland, R. Langer, G. Traverso, *Nat. Mater.* **2015**, *14*, 1065.

[7] Z. Suo, *MRS Bull*. **2012**, *37*, 218.

[8] T. Ware, D. Simon, K. Hearon, C. Liu, S. Shah, J. Reeder, N. Khodaparast, M. P. Kilgard, D. J. Maitland, R. L. Rennaker, W. E. Voit, *Macromol. Mater. Eng.* **2012**, *297*, 1193.

[9] A. de Leon, A. C. Barnes, P. Thomas, J. O'Donnell, C. A. Zorman, R. C. Advincula, *ACS Appl. Mater. Interfaces* **2014**, *6*, 22695.

[10] R. Klajn, M. Fialkowski, I. T. Bensemann, A. Bitner, C. J. Campbell, K. Bishop, S. Smoukov, B. A. Grzybowski, *Nat. Mater.* **2004**, *3*, 729.

[11] J. Mu, C. Hou, B. Zhu, H. Wang, Y. Li, Q. Zhang, *Sci. Rep.* **2015**, *5*, 9503.

[12] a) E. Palleau, D. Morales, M. D. Dickey, O. D. Velev, *Nat. Commun.* **2013**, *4*, 2257; b) B. P. Lee, S. Konst, *Adv. Mater.* **2014**, *26*, 3415.

[13] a) S. Sundaram, D. S. Kim, M. A. Baldo, R. C. Hayward, W. Matusik, *ACS Appl. Mater. Interfaces* **2017**, *9*, 32290; b) Z. Zhao, J. Wu, X. Mu, H. Chen, H. J. Qi, D. Fang, *Sci. Adv.* **2017**, *3*.

[14] a) R. M. Erb, J. S. Sander, R. Grisch, A. R. Studart, *Nat. Commun.* **2013**, *4*, 1712; b) C. Zhang, J.-W. Su, H. Deng, Y. Xie, Z. Yan, J. Lin, *ACS Appl. Mater. Interfaces* **2017**, *9*, 41505; c) H. Deng, Y. Dong, J.-W. Su, C. Zhang, Y. Xie, C. Zhang, M. R. Maschmann, Y. Lin, J. Lin, *ACS Appl. Mater. Interfaces* **2017**, *9*, 30900; d) M. Ma, L. Guo, D. G. Anderson, R. Langer, *Science* **2013**, *339*, 186.

[15] a) A. Schneemann, V. Bon, I. Schwedler, I. Senkovska, S. Kaskel, R. A. Fischer, *Chem. Soc. Rev.* **2014**, *43*, 6062; b) P. Horcajada, F. Salles, S. Wuttke, T. Devic, D. Heurtaux, G. Maurin, A. Vimont, M. Daturi, O. David, E. Magnier, N. Stock, Y. Filinchuk, D. Popov, C. Riekel, G. Férey, C. Serre, *J. Am. Chem. Soc.* **2011**, *133*, 17839; c) C. Serre, C. Mellot-Draznieks, S. Surblé, N. Audebrand, Y. Filinchuk, G. Férey, *Science* **2007**, *315*, 1828; d) S. Surblé, C. Serre, C. Mellot-Draznieks, F. Millange, G. Férey, *ChemComm* **2006**, 284; e) C. Serre, F. Millange, S. Surblé, G. Férey, *Angew. Chem. Int. Ed.* **2004**, *43*, 6285; f) G. Férey, C. Serre, *Chem. Soc. Rev.* **2009**, *38*, 1380; g) C. Mellot-Draznieks, C. Serre, S. Surblé, N. Audebrand, G. Férey, *J. Am. Chem. Soc.* **2005**, *127*, 16273. h) Y. Sakata, S. Furukawa, M. Kondo, K. Hirai, N. Horike, Y. Takashima, H. Uehara, N. Louvain, M. Meilikhov, T. Tsuruoka, S. Isoda, W. Kosaka, O. Sakata, S. Kitagawa, *Science* **2013**, *339*, 193; i) S. Horike, S. Shimomura, S. Kitagawa, *Nat. Chem.* **2009**, *1*, 695.

[16] J. Troyano, A. Carné-Sánchez, J. Pérez-Carvajal, L. León-Reina, I. Imaz, A. Cabeza, D. Maspoch, *Angew. Chem. Int. Ed.* **2018**, *57*, 15420.

[17] a) J. Dechnik, J. Gascon, C. J. Doonan, C. Janiak, C. J. Sumby, *Angew. Chem. Int. Ed.* **2017**, *56*, 9292; b) M. S. Denny Jr., S. M. Cohen, *Angew. Chem. Int. Ed.* **2015**, *54*, 9029.

c) B. Seoane, J. Coronas, I. Gascon, M. E. Benavides, O. Karvan, J. Caro, F. Kapteijn, J. Gascon, *Chem. Soc. Rev.* **2015**, *44*, 2421; d) M. S. Denny, M. Kalaj, K. C. Bentz, S. M. Cohen, *Chem. Sci.* **2018**, *9*, 8842.

[18] a) Z. Wang, P. Dong, Z. Sun, C. Sun, H. Bu, J. Han, S. Chen, G. Xie, *J. Mater. Chem. B* **2018**, *6*, 2426; b) S. Wang, Y. Lv, Y. Yao, H. Yu, G. Lu, *Inorg. Chem. Commun.* **2018**, *93*, 56; c) X. Cai, J. Lin, M. Pang, *Cryst. Growth Des.* **2016**, *16*, 3565.

[19] J. Espín, L. Garzón-Tovar, A. Carné-Sánchez, I. Imaz, D. Maspoch, *ACS Appl. Mater. Interfaces* **2018**, *10*, 9555.

Troyano *et al.*, Figure 1

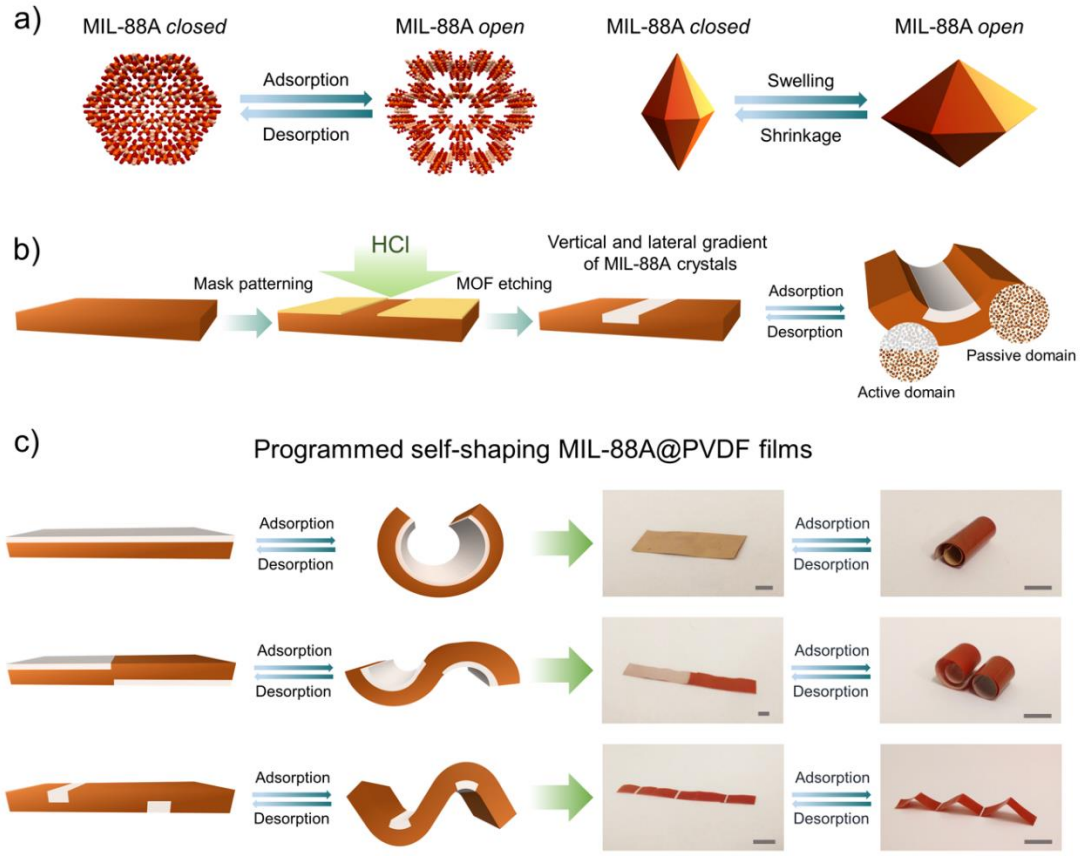

Figure 1. a) Schematic representation of the structural transformation upon adsorption/desorption (left) and resulting swelling/shrinkage (right) of MIL-88A crystals. b) Schematic representation of the patterning of MIL-88A@PVDF films by chemical etching with HCl. c) Schematic (left) and photographs (right) of two different patterned MIL-88A@PVDF films, showing multiaxial actuation. Scale bars = 5 mm.

Troyano *et al.*, Figure 2

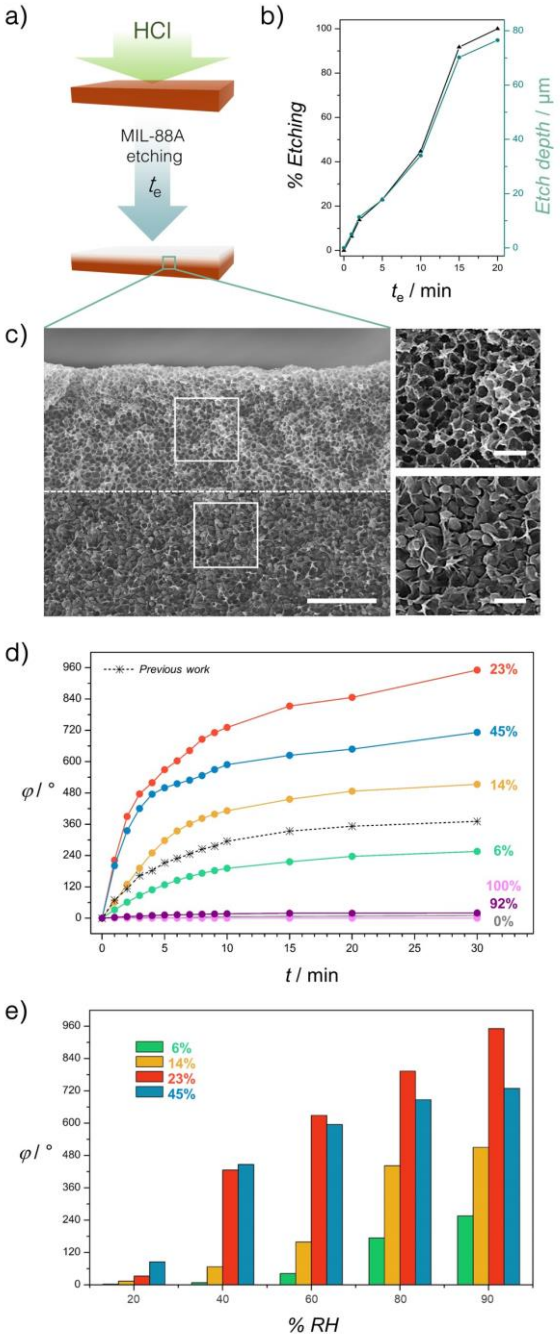

Figure 2. a) Schematic representation of the fabrication of a vertically etched MIL-88A@PVDF film by exposing a homogeneous MIL-88A@PVDF film to HCl for a period of time (t_e). b) Vertical etching extent (%) and etch depth (µm) in function of time. c) Cross-sectional FESEM image of a heterogeneous MIL-88A@PVDF film and magnified images of the MIL-88A containing layer (top right) and PVDF layer (bottom right). Scale bars = 5 µm and 1 µm (magnified). d) Temporal change in the folding angle (φ) of MIL-88A@PVDF strips with different vertical etching extents at 90% relative humidity (RH).[16] e) Folding angle (φ) of MIL-88A@PVDF strips differing by degree of vertical etching (%), after 30 min of exposure to moisture at different values of relative humidity (RH).

Troyano *et al.*, Figure 3

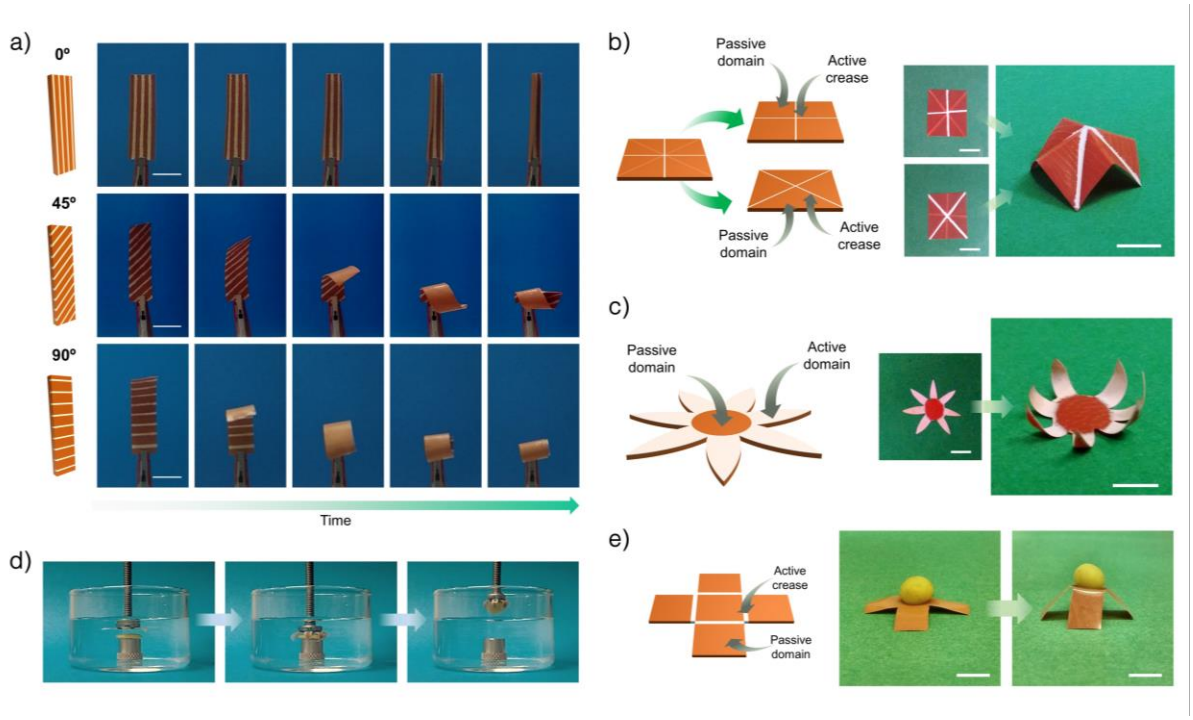

Figure 3. a) Temporal change in the shape of patterned MIL-88A@PVDF strips with parallel etched segments oriented at 0°, 45° or 90° relative to the length axis, upon exposure to 90% relative humidity. Scale bars = 1 cm. b) Schematic (left) and photographs (right) of 3D four-pointed star structure assembled from 2D patterned MIL-88A@PVDF film subjected to 90% relative humidity. Scale bars = 1 cm. c) Schematic (left) and photographs (right) of 3D seven-petal flower structure assembled from 2D patterned MIL-88A@PVDF film and subjected to 90% relative humidity. Scale bars = 5 mm. d) Self-folding claw application of patterned MIL-88A@PVDF seven-petal flower structure, gripping a modeling-clay disc immersed in warm water. e) Schematic (left) and photographs (right) of a patterned MIL-88A@PVDF open-cube structure lifting cargo that is five-times heavier, upon exposure to 90% relative humidity. Scale bars = 5 mm.

Troyano *et al.*, Figure 4

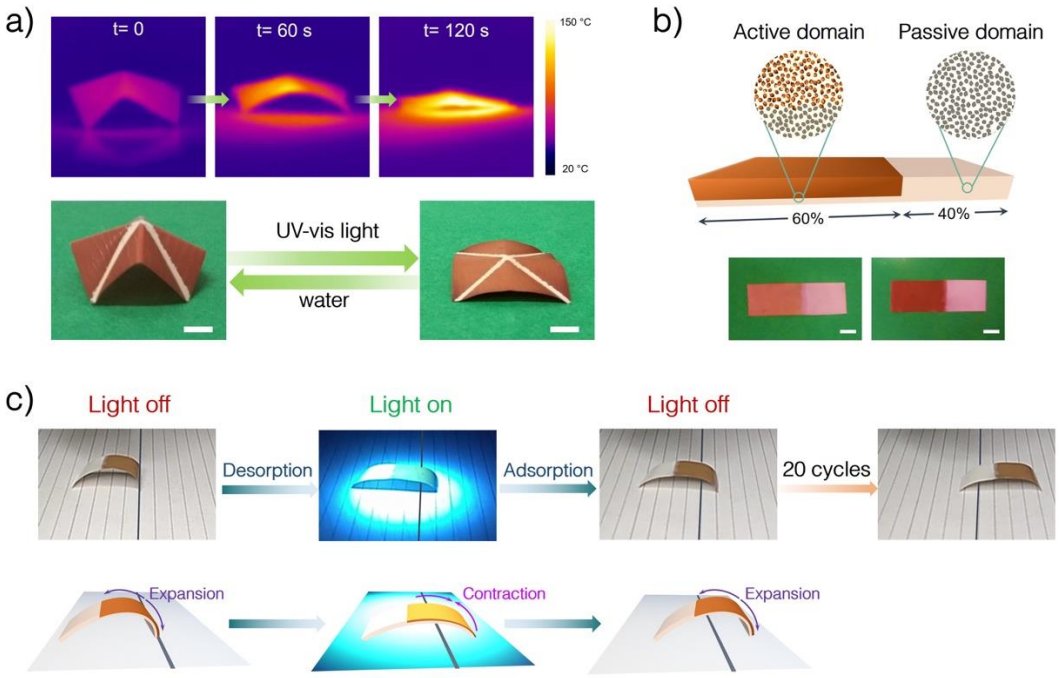

Figure 4. a) Thermographic images (top), and photographs (bottom), of the 3D four-pointed star MIL-88A@PVDF, as it transforms into a planar conformation upon irradiation with UV-Vis light. Scale bars = 5 mm.b) Schematic (top) and photographs (bottom) of the walking motion of a patterned MIL-88A@PVDF strip. c) Photographs (top) and schematic (bottom) of the walking motion of a patterned MIL-88A@PVDF strip in response alternating on/off cycles of UV-Vis irradiation. Interlinear spacing: 5 mm.

Programmable self-shaping composite films are successfully fabricated via controlled chemical etching of swellable MOFs crystals embedded in a polymer matrix. This method allows preparing multiple types of patterned structures, which exhibited enhanced self-folding response and predictable 2D-to-3D shape transformations driven by water adsorption, and which can be reversed by light-induced desorption.

Javier Troyano, Arnau Carné-Sánchez, Daniel Maspoch*

Programmable Self-Assembling 3D Architectures Generated by Patterning of Swellable MOF-based Composite Films